

# Microemulsification-based method enables field-deployable quantification of oil in produced water

Ricardo A.G. de Oliveira<sup>a</sup>, Rogerio M. Carvalho<sup>b</sup>, Angelo L. Gobbi<sup>a</sup>, Renato S. Lima<sup>a,c,d,e,\*</sup>

<sup>a</sup> Brazilian Nanotechnology National Laboratory, Brazilian Center for Research in Energy and Materials, Campinas, Sao Paulo 13083-970, Brazil

<sup>b</sup> Research and Development Center, Leopoldo Américo Miguez de Mello, Petrobras, Rio de Janeiro, RJ, Brazil

<sup>c</sup> Institute of Chemistry, University of Campinas, Campinas, Sao Paulo 13083-970, Brazil

<sup>d</sup> São Carlos Institute of Chemistry, University of Sao Paulo, Sao Carlos, Sao Paulo 09210-580, Brazil

<sup>e</sup> Federal University of ABC, Santo Andre, Sao Paulo 09210-580, Brazil

## ARTICLE INFO

### Keywords:

Rapid test  
Point-of-use  
Microemulsion  
Naked-eye  
Turbidimetry

## ABSTRACT

The oil and gas industry involves the generation of a large amount of produced water (PW), which incorporates chemicals of ecological concern such as petroleum compounds (oil) that further imply deleterious effects to its recovery rate and safety of operation. As limitation, the monitoring of oil in PW (OiW) samples at onshore and offshore wells is challenging as the currently available methods usually require the use of benchtop equipment and laborious experimental routines. Using the microemulsification-based method (MEC), which was introduced by our group in 2014, here we describe a cost-effective, user-friendly, fast, and scalable strategy for the on-field determination of OiW. The analysis is based on the monitoring of the minimum volume fraction of amphiphile needed to thermodynamically stabilize cloudy dispersions, thus forming transparent microemulsions. Applying the own sample as oil-water phases, Tween-80 25% v/v in acetone as amphiphilic phase, and a handheld turbidimeter, the assays are performed in less than 5 min with a limit of detection of ~6 ppm. The latter is lower than the maximum average (OiW 29 ppm per month) that is limited by the Brazilian environmental agency. In addition to showing high robustness facing changes in salinity, it is noteworthy that the method enabled the determination of OiW in real samples with accuracies ranging from 95.7% to 105.6%. Our results are a significant step towards the on-field quantification of OiW. The oil and gas industry may benefit from this method for translating useful solutions into the real world to support the making/management of decisions aiming to minimize ecological and operational side effects.

## 1. Introduction

Formed during the exploration of oil and gas from onshore and offshore wells, the so-called produced water (PW) is composed of formation and injected water along with production chemicals that are originally injected into reservoir to enhance the recovery rate and operation safety [1–4]. PW is the largest stream of waste derived from oil and gas production platforms and its volume further increases with the age of the well [5]. Three barrels of PW are estimated to be generated worldwide for each barrel of extracted oil. In the USA, 300 million barrels of PW were produced in 2016 [6,7]. While treated PW presenting lowered contents of unwanted species is reinjected into reservoirs, its

discharge to the sea is a common management strategy, thus representing a continuous source of contaminants to the ecosystem [4,8].

The aromatic hydrocarbons presented in the dissolved oil in PW may be found out under concentrations enough to cause bioaccumulation and toxicity [5]. In this way, the determination of oil in produced water (OiW) at onshore and offshore wells is key by taking up the large generation of PW and its deleterious effects to the environment and marine animals [4]. In addition to chronic ecological harms, high contents of OiW can lead to pipe obstruction (when PW is reinjected in underground formations) and damages on PW recycling downstream equipment [9], further emphasizing the relevance of the OiW monitoring. Indeed, the OiW content is a key parameter that is historically used by the oil and

**Abbreviations:** PW, produced water; OiW, oil in produced water; MEC, microemulsification-based method; AP, amphiphile;  $\Phi_{ME}$ , minimum volume fraction of AP to form microemulsion;  $V_S$ , volume of sample transferred to the test tube;  $V_{AP}$ , volume of amphiphile added to form microemulsion;  $\Phi_{AP}$ , volume fraction of AP.

\* Corresponding author at: Brazilian Nanotechnology National Laboratory, Brazilian Center for Research in Energy and Materials, Campinas, Sao Paulo 13083-970, Brazil.

E-mail address: [renato.lima@lnnano.cnpem.br](mailto:renato.lima@lnnano.cnpem.br) (R.S. Lima).

<https://doi.org/10.1016/j.fuel.2021.121960>

Received 11 July 2021; Received in revised form 4 September 2021; Accepted 7 September 2021

Available online 28 September 2021

0016-2361/© 2021 Published by Elsevier Ltd.

gas industry for compliance monitoring and reporting to regulatory authorities [5]. Norms defined by environmental agencies limit the amounts of OiW to maximum averages per month, e.g., 29 ppm as established in Brazil [1,10].

Several methods have been applied in the determination of oil in PWs, including gravimetry [11], infrared [8,12,13], fluorescence [8,14], UV–Vis spectrophotometry [15–17], gas chromatography with flame ionization detection [5], and a total organic carbon analyzer [17]. Gravimetry (EPA 1664-A) is one of the most widespread methods and it is based on liquid–liquid extraction utilizing n-hexane. Despite of its low-cost, this technique has disadvantages such as time-consuming operation and poor levels of sensibility and accuracy, which are caused by the loss of components by volatilization and interferences from species extracted by solvent, respectively [17]. Moreover, although valuable by delivering accurate determinations in offshore laboratories, the aforesaid instrumental methods need laborious sample preparation steps and benchtop equipment that inhibit on-field tests. These sample preparation steps further require the use of costly solvents, i.e., S-316 and AK-225. Thus, the development of approaches capable of providing the simple, fast, and reliable analysis of OiW remains a valuable challenge. Further, the online monitoring of this analyte is of interest to the oil and gas industry as it enables the making and management of decisions with more efficacy.

Using the microemulsification-based method (MEC), this paper addresses the determination of OiW in a low-cost, simple, rapid, point-of-use, and scalable fashion. Proposed by our group in 2014 [18–22], MEC is based on the thermodynamic stabilization of water–oil dispersions such as emulsions, forming microemulsions. While this method allowed for naked-eye detection, requiring only test tubes and 1.0-mL plastic syringes, its accuracy was further increased through the use of a hand-held turbidimeter. The assays could be performed in a direct way in less than 5 min per sample and delivered satisfactory precision, linearity, and accuracy for PW real samples. Interestingly, the microemulsions can also be used in the oil industry to remove contents of oil and salinity from PW samples [23,24].

Briefly, the MEC depends on the effect of analyte contents on the entropy of unstable emulsions or Winsor systems, modifying the surface activity (it reduces the interfacial tension) and ultimately varying the minimum volume fraction of amphiphile (AP) needed to form thermodynamically stable microemulsions ( $\Phi_{ME}$ ) at a fixed ratio of water and oil phases.  $\Phi_{ME}$  is the analytical response of the MEC and it can be detected with naked-eyes through the monitoring of cloudy-transparent transition as this process acts as the turning point of the thermodynamic stabilization of dispersions (microemulsification). While the MEC experimental routine is similar to the operation of classic volumetric titrations, its turning point is not associated with chemical reaction-induced alterations in color, but with changes in turbidity because of the emulsion/microemulsion conversion that leads to a cloudy/transparent transition as a function of the droplet size [13].

In the MEC, the analyte can be found in any of the phases of the dispersion, i.e., water, oil, or AP, so that the analytical approach is universal with regard to the polarity of the samples. Here, in contrast to our previous works in which the samples constituted a single phase [18–20], the PW-spiked samples acted simultaneously as water and oil phases. Thus, the method was simplified to 2 components only, i.e., the sample itself and AP that was composed of surfactant and cosurfactant. We assessed different surfactants, cosurfactants, their ratio, and medium salinities. Direct assays based on analytical curves were accomplished both with naked-eyes and with the aid of a turbidimeter for detection of oil in two types of samples: synthetic (spiked with distinct acidic components) and real PW samples.

## 2. Experimental section

### 2.1. Chemicals and material

Hydrochloride acid (HCl), sodium chloride (NaCl), oleic acid, and calcium chloride ( $\text{CaCl}_2$ ) were purchased from Labsynth (Sao Paulo, Brazil). n-Propanol, 1-pentanol, Triton X-100 (TX-100), Tween-80 (TW-80), Tween-20 (TW-20), sodium dodecyl sulfate (SDS), hexadecane, cetyl trimethyl ammonium bromide, acetone (CTBA), ethyl acetate, benzoic acid, stearic acid, and mix of naphthenic acids (MNA) were purchased from Sigma-Aldrich Chemical Co. (St. Louis, MO). Ultra-Turrax (IKA, model T25) and turbidimeter (Digimed, model DU-TU) were used for mixing and response detection, respectively, whereas plastic syringes of 1.0 mL (visual sampling accuracy of 0.02 mL) were purchased from local pharmacies.

### 2.2. Amphiphilic phases

As AP phase, we tested non-ionic (TX-100, TW-80, and TW-20), anionic (SDS), and cationic surfactants (CTAB). The nonionic APs were prepared in different conditions, i.e., diluted in the solvents acetone or ethyl acetate (50% v/v) and diluted in the cosurfactants n-propanol or 1-pentanol. The ionic phases, in turn, were prepared in water (5.0% w/w in water) and, subsequently, diluted in these same media at 1:1 v/v ratio.

### 2.3. OiW standard solutions

Distinct OiW standard solutions were prepared in acetone as shown in Table 1 (OiW<sub>1</sub>, OiW<sub>2</sub>, OiW<sub>3</sub>, MNA, and benzoic acid) and, then added into aqueous media to form synthetic PW samples as described next. Each standard solution was composed of two components, acid and oil. For instance, OiW<sub>1</sub> was composed of oleic acid and hexadecane. The solutions termed OiW<sub>2</sub> and OiW<sub>3</sub> were prepared to contain distinct acids that are also quantified like oil in PW, i.e., stearic acid, benzoic acid, and MNA. The three previous standard solutions were applied in recovery assays. In addition, we studied the sensibility of MEC in the presence of MNA and benzoic acid (Supplementary Information).

### 2.4. Preparation of synthetic PW samples

Synthetic samples were produced simulating the high salinity of PW samples by adding NaCl and  $\text{CaCl}_2$  at different total concentrations (25.0 g L<sup>-1</sup> to 155.0) with a ratio of 10:1 w/w (NaCl to  $\text{CaCl}_2$ ) [17]. Then, aliquots of the OiW standard solution were slowly added into the brine (10.0 to 500.0 ppm) under stirring with the Turrax mixer at 13,000 rpm for 10 min. Subsequently, this speed was reduced to 3000 rpm for 2 min.

### 2.5. Analytical routine

As mentioned before, various media were evaluated as AP phase, whereas the samples constituted both the water and oil phases due to the presence of aqueous brine and oil in their composition. The liquids were

**Table 1**  
Composition of the standard solutions (stock solutions) for simulating OiW.

Standard solution	Concentrations of chemical components	
OiW <sub>1</sub> (10 g L <sup>-1</sup> )	10 g L <sup>-1</sup> oleic acid	10 g L <sup>-1</sup> hexadecane
OiW <sub>2</sub> (10 g L <sup>-1</sup> )	5 g L <sup>-1</sup> benzoic acid	10 g L <sup>-1</sup> hexadecane
	5 g L <sup>-1</sup> oleic acid	
OiW <sub>3</sub> (30 g L <sup>-1</sup> )	10 g L <sup>-1</sup> naphthenic acid	10 g L <sup>-1</sup> hexadecane
	10 g L <sup>-1</sup> oleic acid	
	10 g L <sup>-1</sup> stearic acid	
MNA (10 g L <sup>-1</sup> )	10 g L <sup>-1</sup> naphthenic acid	10 g L <sup>-1</sup> hexadecane
Benzoic acid (10 g L <sup>-1</sup> )	10 g L <sup>-1</sup> benzoic acid	10 g L <sup>-1</sup> hexadecane

sampled and transferred with the aid of 1.0 mL syringes, whereas the detection of the cloudy-transparent transition to achieve  $\Phi_{ME}$  was conducted in two ways, i.e., with naked-eyes and using the turbidimeter.

## 2.6. Naked-eye detection

In practice, 3.0 mL of PW sample were transferred to test tubes containing 0.1 mL of HCl (0.1 M) followed by the addition of AP. After, the tube was closed and shaken using a vortex to accelerate the turbid-transparent transition. The analytical signal of the MEC,  $\Phi_{ME}$  (% v/v), was obtained according to equation [18–20]:

$$\Phi_{ME}(\%) = \frac{V_{AP}}{V_S + V_{AP}} \times 100 \quad (1)$$

In which  $V_{AP}$  refers to the volume of amphiphile added to form microemulsion and  $V_S$  is the volume of sample transferred to the test tube, along with 0.1 mL of HCl (3.1 mL). For a more accurate reading of the transition process by minimizing interference from external lighting, a lightbox containing light-emitting diodes (LED, Fig. S1) was developed to accommodate the sample-with tubes (Supplementary Information).

## 2.7. Turbidimetric detection

The minimum volume required to perform the turbidimeter reading was increased to 5.0 mL of the PW, which was transferred to cuvettes containing 0.17 mL of HCl. After adding the AP, the cuvettes were manually stirred, kept at rest for 20 s to eliminate the air bubbles produced during shaking, and introduced in the equipment for reading.  $\Phi_{ME}$  was calculated from Eq. (1) as well. In this case,  $V_{AP}$  was 5.17 mL. In order to facilitate the data treatment by user, a smartphone app was developed using the Android Studio® software to convert automatically the  $\Phi_{ME}$  values in concentration after simple selection of analysis routine (naked-eye or with turbidimetric detection, Fig. S2) by operator (Supplementary Information).

The samples were acidified (pH 2.5) according to the principle applied by EPA-1664 [11]. This step leads to an increase in the medium ionic strength, thus compressing the electric double layer around the oil droplets and ultimately allowing for their coalescence. In addition, the acidification shifts the ionization balance of carboxylic acids and phenols to their molecular structures that are less hydrophilic than their ionized states. Therefore, the overall solubility of acids (more than 5 carbons) in water is decreased. The two prior phenomena imply an increase in the sample turbidity with resultant improvement in the sensing performance of MEC [25–28].

## 2.8. Study of experimental parameters

First, the MEC response was evaluated using various surfactants (TW-80, TX-100, CTBA, SDS, and TW-20) diluted to 50% v/v and co-surfactants (n-propanol, 1-pentanol, ethyl acetate, and acetone). Were used a synthetic PW sample with 300.0 ppm OiW<sub>1</sub>. The AP phase with the best levels of analytical sensibility (S) and correlation coefficient ( $R^2$ ) was selected to study the surfactant-diluent ratio (25%, 50%, and 75% v/v) by evaluating the method performance from analytical curves at room temperature (~23.0 °C). The S level of the method can be expressed as its ability to discriminate between small differences in analyte concentration. Its value was determined as the slope, i.e., angular coefficient, of the analytical curves ( $\Phi_{ME}$  vs. concentration of oil). The concentrations of OiW ranged initially from 100.0 to 500.0 ppm. Once optimized, the method was applied for lower amounts of OiW<sub>1</sub> (10.0 to 150.0 ppm).

## 2.9. Application to synthetic and real PW samples

Once the ideal AP phase was selected concerning the highest levels of linearity and sensibility, the approach was applied to synthetic PW

samples with distinct compositions, i.e., OiW<sub>1</sub>, OiW<sub>2</sub>, and OiW<sub>3</sub> (Table 1). These samples were prepared following the procedure described in the section 2.4. The resulting recoveries were analyzed by taking up the analytical concentrations as true values.

We further tested the accuracy of the MEC through the analysis of samples provided by the Petrobras (Rio de Janeiro, Brazil). Gravimetric analyses using the protocol EPA 1664-A were performed as our analytical reference method (Supplementary Information). The statistical comparison with the OiW values by MEC were based on Student's t tests at 95% confidence level ( $\alpha = 0.05$ ). The accuracy was determined by the ratio between the oil concentrations reached by the MEC and by the analytical reference method, i.e., gravimetry, that was assumed to produce the true values [29–31]. The recovery has a similar concept to accuracy, but it is applied for standard solutions rather than real samples. The experiments were conducted at 23 °C and pH 2.5.

## 3. Results and discussion

### 3.1. Evaluation of amphiphilic phases

Fig. 1A illustrates how the MEC worked to quantify oil in PW samples. Microemulsification occurred as a function of the adsorption of AP on water–oil interfaces of PW samples. Such phenomenon creates a surface pressure ( $\pi$ ) that decreases the interface tension ( $\gamma_i$ ) as described below [21]:

$$\gamma_i = \gamma_0 - \pi \quad (2)$$

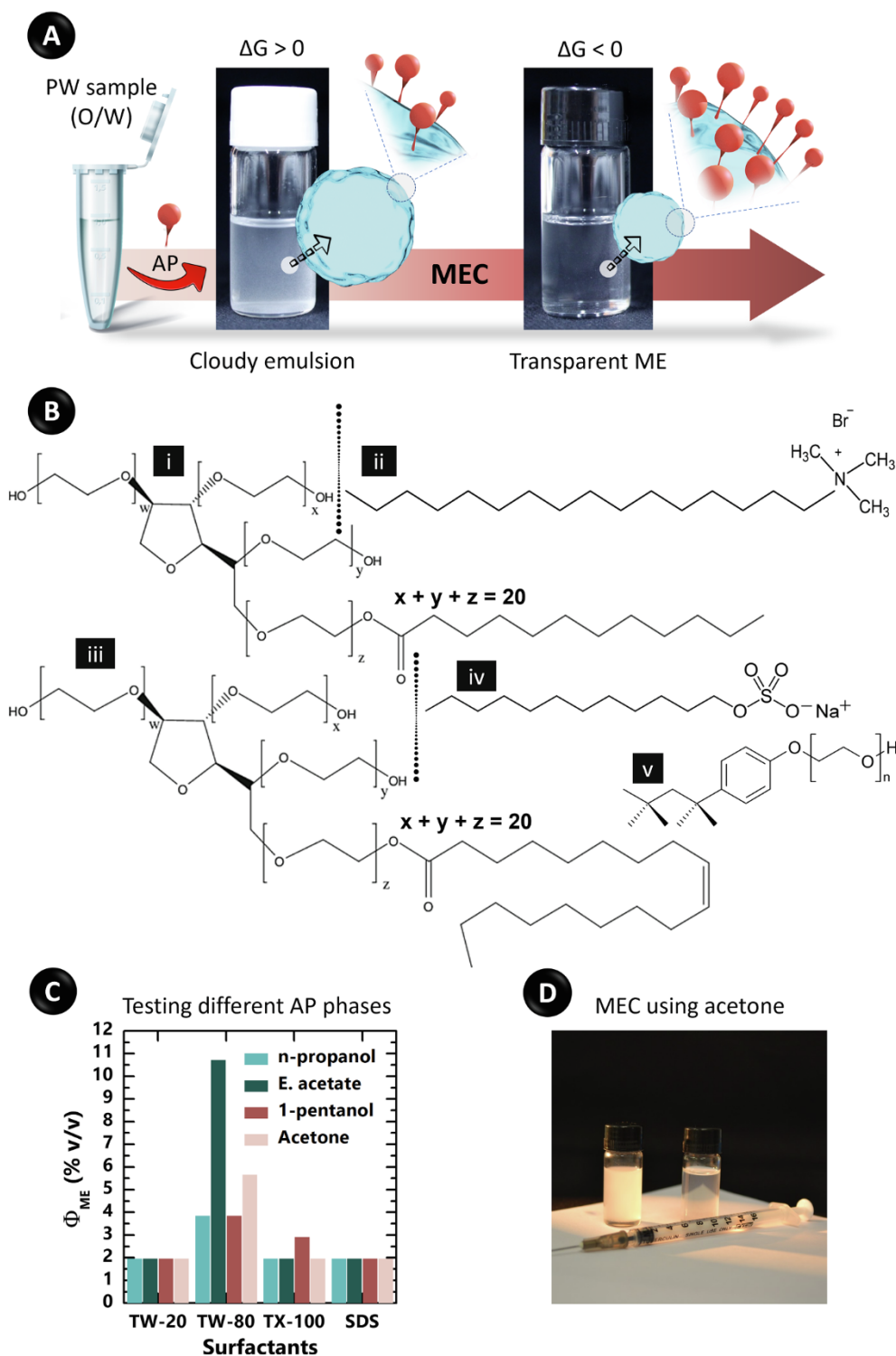
In which  $\gamma_0$  means the interface tension before adding AP. Ultimately, the reduction in  $\gamma_i$  with addition of AP leads to thermodynamic stabilization of emulsions by decreasing Gibbs free energy [21,22]. Microemulsions also differ from emulsions in droplet size. The hydrodynamic diameters of the droplets dispersed in emulsions range from 1 to 10  $\mu$ m. Thereby, such droplets are able to scatter the visible light, creating cloudy media. In contrast, this parameter presents a maximum value of only ~300 nm in microemulsions due to the increase in  $\pi$ , with consequent formation of transparent media [18]. This cloudy-transparent transition with microemulsification allowed for the detection of  $\Phi_{ME}$  in PW samples.

Fig. 1B shows the structures of the tested surfactants, which were diluted in different media among cosurfactants (n-propanol and 1-pentanol) and solvents (ethyl acetate and acetone) as aforesaid. The analyses were made with naked-eye detection to a synthetic PW sample with high oil concentration, i.e., 300.0 ppm OiW<sub>1</sub>. In this regard, since the OiW amount can reach values as low as 1.0 ppm in real conditions, the goal of this study was to select the surfactant with the lower microemulsification efficiency (highest  $\Phi_{ME}$ ). Otherwise, the AP volumes to be added in these low-concentration cases would be too low to be accurately sampled via simple and low-cost plastic syringes.

For most cases, APs showed high efficiency in the formation of microemulsions from emulsions as illustrated in Fig. 1C. The values of  $\Phi_{ME}$  found for TW-20, TX-100, and SDS were on the order of 2.0% v/v. The high surface activities presented by these surfactants reflect their enhanced ability in adsorbing on water–oil interfaces and ultimately reducing  $\gamma_i$ , thus favoring the thermodynamic stabilization of dispersions [21]. As consequence, low values of  $\Phi_{ME}$  are needed for microemulsification as observed.

The high efficiency of TX-100 is owing to its branched chain that increases the number of molecular conformations and lateral interactions at water–oil interfaces [23]. The high surface activity presented by SDS and TW-20, in turn, are associated with the small size of their polar and nonpolar groups, respectively, by allowing for a dense packaging of the amphiphile molecules at water–oil interfaces [24,25].

CTAB did not result in the formation of microemulsions, while TW-80 showed the highest  $\Phi_{ME}$  values for all the investigated co-surfactants. This low efficiency is likely due to the presence of a central cis C=C double bond in TW-80 carbon chain (see Fig. 1B) by showing



**Fig. 1.** Principle and surfactants. (A) MEC operation to determine oil in a sample of PW. (B) Molecular structures of surfactants: TW-20 (i), CTAB (ii), TW-80 (iii), SDS (iv), and TX-100 (v). (C) Data of  $\Phi_{ME}$  for different surfactant-diluent sets that were applied to PW samples with 300.0 ppm OiW<sub>1</sub>. (D) Photo of the transition from cloudy (on left) to transparent dispersion (on right) bearing OiW<sub>1</sub> and TW-80 25% v/v in acetone. In (A), G means the Gibbs free energy.

stereochemical restrictions that hinder its curvature at water-oil interfaces and ultimately decrease  $\pi$  [26].

When compared with the media in acetone and ethyl acetate, the TW-80 solutions diluted in n-propanol and 1-pentanol generated lower values of  $\Phi_{ME}$ . This result is in agreement with the amphiphilic nature of these alcohols, further increasing  $\pi$ . Such species join the water-oil interfaces placing itself between the surfactant heads, decreasing the

repulsion between the surfactant's long hydrophobic tails and, then enhancing the surface activity [27–29]. TW-80 solutions were chosen as AP phase for the subsequent analyses as they afforded the lowest efficiency of microemulsification. Fig. 1D displays cloudy emulsion and transparent microemulsion containing OiW<sub>1</sub> and TW-80 25% v/v in acetone.

### 3.2. Ideal surfactant-diluent proportion

We next evaluated the effect of the surfactant-diluent proportion on the analytical sensibility by naked-eye detection, which was made with the aid of a lightbox as shown in Fig. 2A. In this lightbox, two tubes were inserted, one with the sample (on the right) and the other with brine solution (on the left) to serve as a reference. The LED's light amplifies the turbidity of the sample while microemulsification is not yet completed, facilitating the visualization of the cloudy-transparent transition.

The TW-80-diluent proportions of 25%, 50% and 75% v/v were

tested. Analytical curves were constructed for each proportion ranging the concentration of oil from 100.0 to 500.0 ppm ( $n = 10$ ). The resulting data of  $S$  and  $R^2$  are shown in Table 2. Poor performance was achieved when using ethyl acetate. The highest values of  $S$  by the AP solutions prepared in the presence of *n*-propanol and 1-pentanol were, respectively, calculated as 0.041% (25% v/v,  $R^2 = 0.99$ ) and 0.048% v/v ppm<sup>-1</sup> (75% v/v,  $R^2 > 0.99$ ). The best condition was attained via the use of TW-80 25% v/v in acetone (0.063% v/v ppm<sup>-1</sup>,  $R^2 = 0.99$ ). Therefore, this amphiphile was chosen for the following measurements. In terms of the use of plastic syringes for sampling and discharging the liquids, although their rubber plungers can be attacked by organic

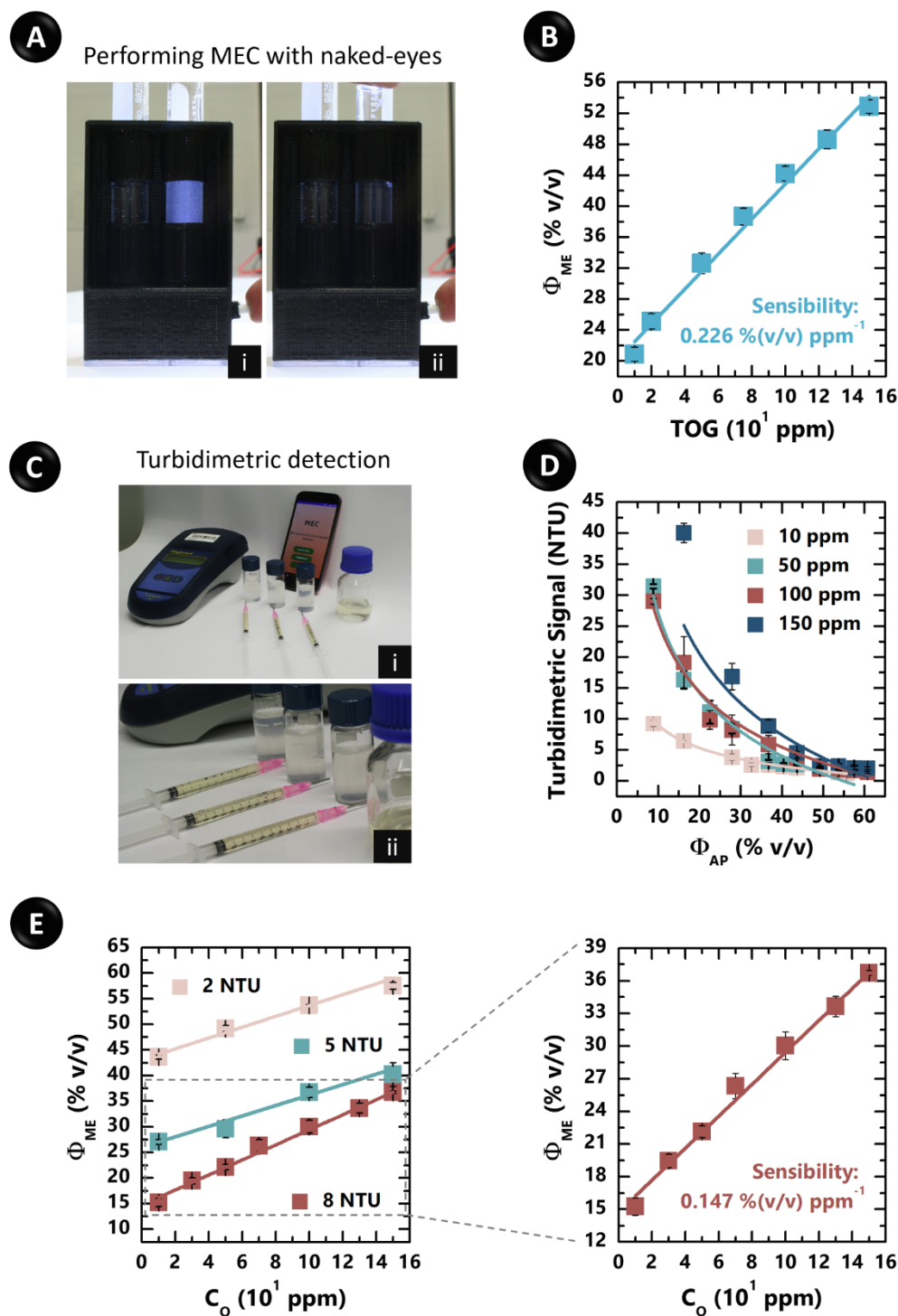


**Fig. 2.** Surfactant-diluent ratio and turbidimetry. (A) Lightbox to make MEC analysis with NE detection with cloudy (i) and transparent dispersion (ii). (B) Analytical curve for OiW<sub>1</sub> using TW-80 25% v/v in acetone. C<sub>O</sub> means concentration of oil. (C) Platform to measure turbidity comprising turbidimeter, cuvettes, syringes, AP, and smartphone (i,ii) with app for converting Φ<sub>ME</sub> in oil content. (D) Values of turbidity as a function of Φ<sub>AP</sub> for OiW<sub>1</sub> samples in different values of C<sub>O</sub>. (E) Analytical curves for OiW<sub>1</sub> utilizing TW-80 25% v/v for different turbidimetric signals as indicative of the cloudy-transparent transition. Inset: amplified view of the analytical curve for an output of 8.1 (±0.2) NTU to detect Φ<sub>ME</sub>.

**Table 2**

Summary of the sensibility results (%v/v ppm<sup>-1</sup> oil) and R<sup>2</sup> for each ratio of TW-80 in different diluents.

Diluent	Proportion (v/v)	Sensibility (10 <sup>-2</sup> )	R <sup>2</sup>
n-Propanol	25%	4.1	0.99
	50%	3.7	0.95
	75%	2.1	0.90
1-Pentanol	25%	2.3	0.90
	50%	0.7	0.66
	75%	4.8	0.99
Acetone	25%	6.3	0.99
	50%	4.1	0.98
	75%	4.5	0.93
Ethyl Acetate	25%	NA	NA
	50%	3.0	0.90
	75%	2.9	0.98

solvents, they were employed in a disposable way. Hence, these syringes had no adverse impact on the method accuracy as indicated by the data to real samples. Anyway, the application of the MEC with the aid of a micropipette is totally feasible.

The analytical curve related to the use of TW-80 25% v/v in acetone for OiW<sub>1</sub> ranging from 10.0 to 130.0 ppm is depicted Fig. 2B (the other curves are presented in Fig. S3). Its sensibility was higher than the value previously reported for the range of 100.0 to 500.0 ppm, reaching 0.226% v/v ppm<sup>-1</sup> with R<sup>2</sup> > 0.99. Impressively, the MEC was able to monitor oil concentrations lower than the monthly average (29 ppm) that is allowed by the Brazilian environmental agency [1,10].

### 3.3. Turbidimetric detection

Once the MEC analysis is based on a drastic reduction in turbidity, an alternative to detect its endpoint is to use a turbidimeter (unit of its signal: nephelometric turbidity unit, NTU) as it was used here. This equipment is supposed to enable more accurate determinations by eliminating possible operator errors. Fig. 2C displays the setup that consisted of turbidimeter, plastic syringes, AP, and cuvettes. Fig. 2D exhibits the turbidity profile at different amounts of OiW<sub>1</sub> (10.0 up to 150.0 ppm, *n* = 6) as the AP (TW-80 25% v/v in acetone) is added gradually. The turbidity decreased nonlinearly with the volume fraction of AP ( $\Phi_{AP}$ ), achieving a plateau region from 45% of  $\Phi_{AP}$  and, then remaining constant (Table S1 shows the equations for the NTU vs.  $\Phi_{AP}$  plots at each concentration of OiW<sub>1</sub>).

To achieve the highest sensibility, three NTU responses were assessed as endpoints to detect  $\Phi_{ME}$ , i.e., the cloudy-transparent transition tied to microemulsification, namely, 2.0, 5.0 and 8.0 NTU. In these cases, the AP was added until these NTU values were reached. Analytical curves were constructed for each output in the concentration range from 10.0 to 150.0 ppm of OiW<sub>1</sub> as exhibited in Fig. 2E. The values of sensibility were 10.2 (2.0), 10.6 (5.0), and 14.7% 10<sup>-2</sup> v/v ppm<sup>-1</sup> (8.0 NTU). In addition to lower sensibilities, the responses 2.0 and 5.0 NTU led to a higher consumption of AP and poorer detectability. The limits-of-detection (LODs) were revealed to be 5.3 (2.0), 6.1 (5.0), and 5.8 ppm (8.0 NTU). In this way, turbidimetric signals equal to  $8.1 \pm 0.2$  NTU were considered as indicatives for measuring the MEC analytical response in the following measurements. One should also underline these LODs are below the monthly maximum average (29 ppm) [1,10].

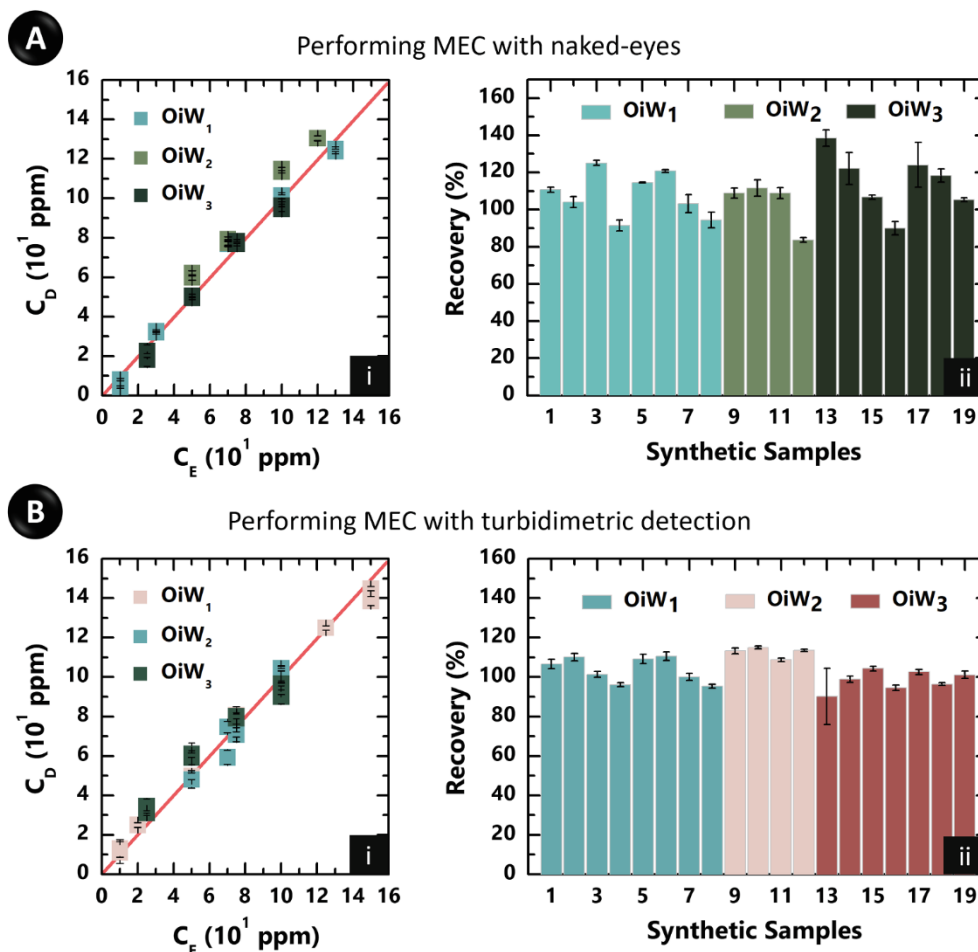


**Fig. 3.** Application to synthetic samples. (A) Parity plot of determined ( $C_D$ ) vs. expected ( $C_E$ ) concentrations of oil (i) and recovery data attained with NE detection to samples spiked with OiW<sub>1</sub>, OiW<sub>2</sub> and OiW<sub>3</sub> as indicated (ii). (B) Plot of  $C_D$  vs.  $C_E$  (i) and recovery values using the turbidimeter to the same samples (ii).

### 3.4. Application to synthetic and real PW samples

The MEC was applied to samples with distinct levels of complexity. A total of 19 PW synthetic samples distributed into three groups with the standard media OiW<sub>1</sub>, OiW<sub>2</sub>, or OiW<sub>3</sub> (Table 1) ranging from 10.0 up to 150.0 ppm were first tested. The results when using naked-eye detection ( $n = 10$ ) are depicted in Fig. 3A. The parity plot of determined vs. expected values (analytical concentrations, i.e., true data) revealed a slope of 0.931 with prediction mean accuracy,  $R^2$ , and mean absolute error (MAE) calculated as 93.1%, 0.98, and 0.153 ppm, respectively. However, the recovery percentages varied from 83.7% up to values larger than 120.0% for 5 samples, mainly for those ones prepared with the more complex standard, OiW<sub>3</sub>. We hypothesized such result is ascribed to the presence of a mix of naphthenic acids, MNA, in this synthetic sample. Preliminary studies revealed that these compounds lead to a sensitive increase in the visual MEC responses. Nonetheless, these inaccurate results were solved by the use of turbidimetry as discussed next.

From Fig. 3B, the turbidimetric MEC signals afforded a parity plot with slope of 1.077, prediction mean accuracy of 107.7%,  $R^2$  of 0.98, and MAE of 32.3 ppb only ( $n = 6$ ). The latter is approximately 5-fold lower than the error obtained for visual detection. In addition, the recovery data showed less dispersion around 100% when compared with naked-eye detection, reaching percentages from 90.1% up to 115.4% with an overall average of  $101.1\% \pm 5.7\%$ . It is also noteworthy that even the complex OiW<sub>3</sub>-with samples could be analyzed with an overall recovery of  $101.1\% \pm 5.7\%$ .

We next evaluated the MEC robustness facing variations in the salinity of PW synthetic samples, which were prepared from 50 ppm OiW<sub>1</sub> at distinct amounts of NaCl and CaCl<sub>2</sub> salts (25 to 155 g L<sup>-1</sup>). It is worth mentioning that the salt proportion adopted in the other studies was maintained (NaCl/CaCl<sub>2</sub> 10:1 w/w). Based on Fig. 4, the oil contents obtained from analytical curve (Fig. 2E, 8.0 NTU) exhibited values above the analytical concentration, varying between 53.6 and 59.8 ppm with resulting recoveries from 107.3% to 119.3%, respectively ( $n = 10$ ). Nevertheless, any type of trend with the salt concentrations was not observed, signaling the MEC can be directly applied to the samples without the need to adjust experimental parameters for salinity correction or to use the standard addition method. This robustness of the method facing changes in the salt concentration is likely due to the nonionic nature of the amphiphile TW-80. In this case, the surface pressure formed by this AP is supposed to undergo only subtle variations after interaction with the ions in the dispersion.

For routine assays, it is crucial to understand the testing performance in complex samples. We thereby challenged the MEC with both naked-eye and turbidimetric detection in 6 real samples provided by

Petrobras. According to data for 4 PW samples derived from the same production field where the samples investigated herein were collected (Fig. S4), these waters are specially enriched in the ions chloride, sodium, bicarbonate, calcium, magnesium, and potassium. In comparison with a standard method (gravimetry), while visual detection suffered from poor accuracy in some cases, the use of turbidimetry provided accurate determinations. The contents of oil by gravimetry varied from 39.2 up to 204.4 ppm. From parity plots in Fig. 5A, the parameters of slope, mean accuracy of prediction,  $R^2$ , and MAE were determined, respectively, as 0.985, 98.5%, 0.97, and 74.9 ppb for naked-eye detection ( $n = 10$ ) and 0.941, 94.1%, 0.99, and 8.34 ppb when using turbidimetric detection ( $n = 6$ ). Fig. 5B exhibits a picture of the scrutinized samples. According to Fig. 5C, the visual detection led to accuracies from 66.8% to 123.4%. Such discrepancies in relation to the gravimetric data can be univocally ascribed to the difficulty in precisely detecting the cloudy-transparent turning points with naked-eyes in these samples to get  $\Phi_{ME}$ . In contrast, the accomplishment of MEC with turbidimetry provided results in consistence with the data reached by gravimetry, with accuracies ranging from 95.7% to 105.3%. When compared with the naked-eye sensing, one should also emphasize that the turbidimetric detection presented a poorer precision (as indicated by the error bars in Fig. 5C) likely because of its higher sensibility, making the analyses more susceptible to a variable interference from particulate material found in the bulk of the dispersions. Another possible and complementary reason is the tendency of the analyst to be influenced to add close AP volumes for the succeeding replicates after the first one when visually performing the detection.

## 4. Conclusion

In this work, MEC proved to be a rapid, user-friendly, field-employable, low-cost, and accurate method to quantify oil in samples of produced water. Using the own PW sample as oil-water phases, TW-80 25% v/v in acetone as AP phase for microemulsification, a handheld turbidimeter, testing tubes, and plastic syringes, the measurements could be performed in less than 5 min without interference from external lightning. Furthermore, the method was found to be robust facing variations in the salinity of the sample, which is particularly important given its variability in realistic sceneries. In this regard, we believe the method presented herein can help to pave the way for the development of sensing solutions capable of delivering the on-field monitoring of OiW. In fact, the approach meets the demands for commercial development, basically requiring off-the-shelf reagents and a handheld turbidimeter. The oil and gas industry may benefit from MEC to prevent unconformities that may be harmful to its productivity, safety of operation, and the environment.

Although the above results are a promising indicator, applications to large-scale samples need to be made further for scrutinizing the applicability of the method. In this way, in contrast to other OiW sensing methods, one should underline that MEC is expected to deliver high-accuracy data as it does not involve extraction procedures for sample preparation before detection. However, one should emphasize that the real samples evaluated herein are from the same production field and they did not show any color that could impair the accuracy of the OiW data. Thus, the application of the method to a collection of several samples is indeed mandatory for probing if a same analytical curve could be universally applied or if a set of curves would be demanded for certain categories of samples. Alternatively, the standard addition method could be required. Efforts should also be devoted to assess the effect of temperature over the MEC performance. A comprehensive understanding of this effect is essential to assist the development of valuable tools that can be translated into the real world for daily applications. Importantly, prior applications revealed that the MEC was able to quantify ethanol in colored real samples via analytical curves [20,22], thus suggesting the microemulsification is not necessarily impaired by the incidence of colored samples. Further, the method was

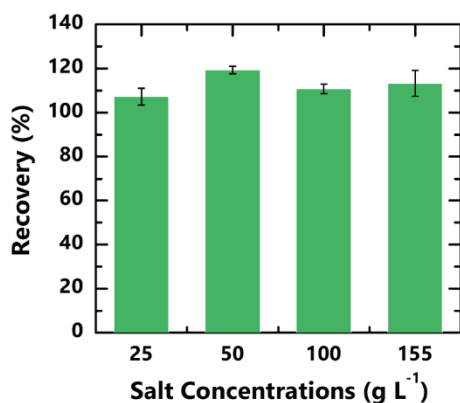
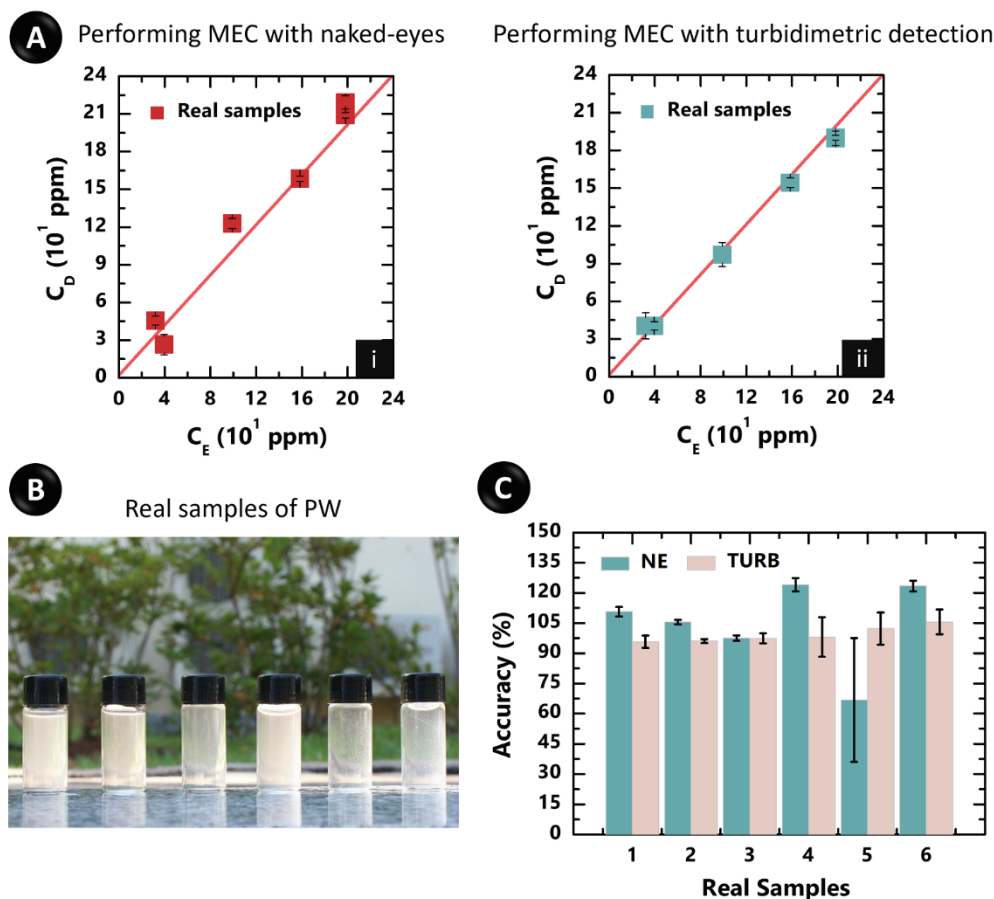


Fig. 4. Investigation of the MEC performance against variations in the sample salinity. Recovery values related to the concentrations of oil obtained by the method for a synthetic sample containing 50 ppm OiW<sub>1</sub> at distinct concentrations of NaCl and CaCl<sub>2</sub> as indicated.



**Fig. 5.** Application to real samples. (A) Plots of  $C_D$  vs.  $C_E$  of oil with NE detection (i) and turbidimeter (ii). (B) Photo of the samples of PW placed from '1' to '6' (left to right) as indicated throughout this work. (C) Accuracy data with NE detection and using the turbidimeter (TURB).

robust facing changes in temperature (18–35 °C) [20].

#### Author contributions

R.S.L. and R.A.G.O. were responsible for the conceptualization of the sensing strategy. All the authors contributed to define the methodology. R.A.G.O. performed the data curation, formal analysis, investigation, and validation. R.M.C. provided the real samples and their characterization. Project administration and supervision were made by R.S.L and A.L.G., whereas R.S.L and R.A.G.O. wrote the original draft of the manuscript. All the authors discussed the results and edited/reviewed the manuscript.

#### Declaration of Competing Interest

The authors declare that they have no known competing financial interests or personal relationships that could have appeared to influence the work reported in this paper.

#### Acknowledgments

Financial support for this project was provided by Petrobras (Grant Nr. 2018/00363-0). Iris R. Sousa Ribeiro, Karen M. Higa, and Rui Mürer are also thanked for helping us with drawings, tests, and prototyping processes, respectively.

#### Appendix A. Supplementary data

Supplementary data to this article can be found online at <https://doi.org/10.1016/j.fuel.2021.121960>.

#### References

- [1] Fakhru'l-Razi A, Pendashteh A, Abdullah LC, Biak DRA, Madaeni SS, Abidin ZZ. Review of technologies for oil and gas produced water treatment. *J Hazard Mater* 2009;170(2-3):530–51. <https://doi.org/10.1016/j.jhazmat.2009.05.044>.
- [2] Amini S, Mowla D, Golkar M, Esmaeilzadeh F. Mathematical modelling of a hydrocyclone for the down-hole oil–water separation (DOWS). *Chem Eng Res Des* 2012;90(12):2186–95. <https://doi.org/10.1016/j.cherd.2012.05.007>.
- [3] Kuttyathil MS, Mohamed MM, Al-Zuhair S. Using microalgae for remediation of crude petroleum oil–water emulsions. *Biotechnol Progr* 2020:e3098. <https://doi.org/10.1002/btpr.3098>.
- [4] Beyer J, Goksøyr A, Hjermann DØ, Klungsoyr J. Environmental effects of offshore produced water discharges: a review focused on the Norwegian continental shelf. *Marine Environ Res* 2020;162:105155. <https://doi.org/10.1016/j.marenvres.2020.105155>.
- [5] Lee K, Neff JM, eds., *Produced water: environmental risks and advances in mitigation technologies*, Springer-Verlag, New York, 2011. <https://doi.org/10.1007/978-1-4614-0046-2>.
- [6] Piotrowski PK, Tasker TL, Geeza TJ, McDevitt B, Gillikin DP, Warner NR, et al. Forensic tracers of exposure to produced water in freshwater mussels: a preliminary assessment of Ba, Sr, and cyclic hydrocarbons. *Sci Rep* 2020;10(1). <https://doi.org/10.1038/s41598-020-72014-6>.
- [7] Dolan FC, Cath TY, Hogue TS. Assessing the feasibility of using produced water for irrigation in Colorado. *Sci Total Environ* 2018;640–641:619–28. <https://doi.org/10.1016/j.scitotenv.2018.05.200>.
- [8] Motta A, Borges C, Esquerre K, Kiperstok A. Oil produced water treatment for oil removal by an integration of coalescer bed and microfiltration membrane processes. *J Membr Sci* 2014;469:371–8. <https://doi.org/10.1016/j.memsci.2014.06.051>.
- [9] Simms K, Zaidi A, Bhargava O. A protocol for determining oil and grease in produced waters. In: Ray JP, Engelhardt FR, editors. *Produced water: technological/environmental issues and solutions*. US, Boston, MA: Springer; 1992. p. 455–71. [https://doi.org/10.1007/978-1-4615-2902-6\\_36](https://doi.org/10.1007/978-1-4615-2902-6_36).
- [10] BRASIL, Conselho Nacional do Meio Ambiente (CONAMA), Resolução n° 393/2007, 2011. <http://www2.mma.gov.br/port/conama/res/res07/res39307.pdf> (accessed September 10, 2019).

- [11] Method 1664, Revision B: n-Hexane Extractable Material (HEM; Oil and Grease) and Silica Gel Treated n-Hexane Extractable Material (SGT-HEM; Non-polar Material) by Extraction and Gravimetry, (n.d.) 35.
- [12] Roy G, Mielczarski JA. Infrared detection of chlorinated hydrocarbons in water at ppb levels of concentrations. *Water Res* 2002;36(7):1902–8. [https://doi.org/10.1016/S0043-1354\(01\)00371-2](https://doi.org/10.1016/S0043-1354(01)00371-2).
- [13] Ramsey ED. Determination of oil-in-water using automated direct aqueous supercritical fluid extraction interfaced to infrared spectroscopy. *J Supercritical Fluids* 2008;44(2):201–10. <https://doi.org/10.1016/j.supflu.2007.10.005>.
- [14] Ehrhardt M, Knap A. A direct comparison of UV fluorescence and GC/MS data of lipophilic open-ocean seawater extracts. *Mar Chem* 1989;26(3):179–88. [https://doi.org/10.1016/0304-4203\(89\)90001-7](https://doi.org/10.1016/0304-4203(89)90001-7).
- [15] Winkler I, Agapova N. Determination of water pollution by the oil products through UV photometry. *Environ Monit Assess* 2010;168(1-4):115–9. <https://doi.org/10.1007/s10661-009-1095-2>.
- [16] Banan Khorshid Z, Mahdi Doroodmand M, Abdollahi S. UV-Vis. spectrophotometric method for oil and grease determination in water, soil and different mediates based on emulsion. *Microchem J* 2021;160:105620. <https://doi.org/10.1016/j.microc.2020.105620>.
- [17] Costa JA, Farias NC, Queirós YGC, Mansur CRE. Determination of oil-in-water using nanoemulsions as solvents and UV visible and total organic carbon detection methods. *Talanta* 2013;107:304–11. <https://doi.org/10.1016/j.talanta.2013.01.040>.
- [18] Lima RS, Shiroma LY, Teixeira AVNC, de Toledo JR, do Couto BC, de Carvalho RM, et al. Microemulsification: an approach for analytical determinations. *Anal Chem* 2014;86(18):9082–90. <https://doi.org/10.1021/ac5025914>.
- [19] da Cunha JG, Shiroma LY, Giordano GF, Couto BC, Carvalho RM, Gobbi AL, et al. Microemulsification-based method: analysis of monoethylene glycol in samples related to natural gas processing. *Energy Fuels* 2015;29(9):5649–54. <https://doi.org/10.1021/acs.energyfuels.5b01166>.
- [20] Giordano GF, Shiroma LY, Gobbi AL, Kubota LT, Lima RS. Microemulsification-based method: analysis of ethanol in fermentation broth of sugar cane. *Anal Methods* 2015;7(23):10061–6. <https://doi.org/10.1039/C5AY02152A>.
- [21] Giordano GF, Higa KM, Santinon A, Gobbi AL, Kubota LT. Microemulsification-based method: coupling with separation technique. *J Anal Bioanal Techniques* 2015;6. <https://doi.org/10.4172/2155-9872.1000261>.
- [22] Higa KM, de Camargo CL, Giordano GF, Silva IPO, Gobbi AL, Kubota LT, et al. Intervening factors in the performance of a naked-eye microemulsification-based method and improvements in analytical frequency. *Anal Methods* 2017;9(22):3347–55. <https://doi.org/10.1039/C7AY00795G>.
- [23] Souza JSB, Ferreira Júnior JM, Simonelli G, Souza JR, Góis LMN, Santos LCL. Removal of oil contents and salinity from produced water using microemulsion. *J Water Process Eng* 2020;38:101548. <https://doi.org/10.1016/j.jwpe.2020.101548>.
- [24] da Silva DC, dos Santos Lucas CR, de Moraes Juviano HB, de Alencar Moura MCP, Dantas Neto AA, de Castro Dantas TN. Novel produced water treatment using microemulsion systems to remove oil contents. *J Water Process Eng* 2020;33:101006. <https://doi.org/10.1016/j.jwpe.2019.101006>.
- [25] EPA, Method 1664, Revision A: n-Hexane Extractable Material (HEM; Oil and Grease) and Silica Gel Treated n-Hexane Extractable Material (SGT-HEM; Non-polar Material) by Extraction and Gravimetry, (1999) 35.
- [26] Kanak AA, Grisard PJ. Deoiling of produced water by acidification. *OnePetro* 1980. <https://doi.org/10.2118/80-31-30>.
- [27] Bertheussen A, Simon S, Sjöblom J. Equilibrium partitioning of naphthenic acid mixture, part 1: commercial naphthenic acid mixture. *Energy Fuels* 2018;32(7):7519–38. <https://doi.org/10.1021/acs.energyfuels.8b01494>.
- [28] Kemmer FN. *Nalco chemical company, the NALCO water handbook*. 2nd ed. McGraw-Hill Inc; 1987.
- [29] Marson BM, Concentino V, Junkert AM, Fachi MM, Vilhena RO, Pontarolo R. Validation of analytical methods in a pharmaceutical quality system. *Quím Nova* 2020;43:1190–203. <https://doi.org/10.21577/0100-4042.20170589>.
- [30] Anonymous, ICH Q2 (R1) Validation of analytical procedures: text and methodology, European Medicines Agency. (2018). <https://www.ema.europa.eu/en/ich-q2-r1-validation-analytical-procedures-text-methodology> (accessed September 1, 2021).
- [31] Peris-Vicente J, Esteve-Romero J, Carda-Broch S. Validation of Analytical Methods Based on Chromatographic Techniques: An Overview, in: *Analytical Separation Science*, American Cancer Society, 2015: pp. 1757–1808. <https://doi.org/10.1002/9783527678129.assep064>.